

A circumstellar dust disk around T Tau N: Sub-arcsecond imaging at $\lambda = 3$ mm

R.L. Akeson,¹ D.W. Koerner,² & E.L.N. Jensen³

ABSTRACT

We present high-resolution imaging of the young binary, T Tauri, in continuum emission at $\lambda=3$ mm. Compact dust emission with integrated flux density 50 ± 6 mJy is resolved in an aperture synthesis map at $0''.5$ resolution and is centered at the position of the optically visible component, T Tau N. No emission above a 3σ level of 9 mJy is detected $0''.7$ south of T Tau N at the position of the infrared companion, T Tau S. We interpret the continuum detection as arising from a circumstellar disk around T Tau N and estimate its properties by fitting a flat-disk model to visibilities at $\lambda = 1$ and 3 mm and to the flux density at $\lambda = 7$ mm. Given the data, probability distributions are calculated for values of the free parameters, including the temperature, density, dust opacity, and the disk outer radius. The radial variation in temperature and density is not narrowly constrained by the data. The most likely value of the frequency dependence of the dust opacity, $\beta = 0.53_{-0.17}^{+0.27}$, is consistent with that of disks around other single T Tauri stars in which grain growth is believed to have taken place. The outer radius, $R = 41_{-14}^{+26}$ AU, is smaller than the projected separation between T Tau N and S, and may indicate tidal or resonance truncation of the disk by T Tau S. The total mass estimated for the disk, $\log(M_D/M_\odot) = -2.4_{-0.6}^{+0.7}$, is similar to masses observed around many single pre-main-sequence sources and, within the uncertainties, is similar to the minimum nebular mass required to form a planetary system like our own. This observation strongly suggests that the presence of a binary companion does not rule out the possibility of formation of a sizeable planetary system.

Subject headings: circumstellar matter — stars:pre-main sequence — star:individual (T Tauri)

¹Radio Astronomical Laboratory, UC Berkeley, Berkeley, CA 94720

²University of Pennsylvania, Dept. of Physics & Astronomy, 209 S. 33rd St., Philadelphia, PA 19104-6396

³Dept. of Physics & Astronomy, Arizona State University, Tempe, AZ 85287-1504

1. Introduction

Circumstellar material, generally believed to be in the form of disks, is detected around most T Tauri stars (Strom et al. 1989; Beckwith et al. 1990). A comparison of inferred disk properties with theoretical constructions suggests that these disks play a dual role as a source of accretion material for star formation (Shu et al. 1993) and a reservoir of material from which planetary systems may arise (cf. Beckwith & Sargent 1996; Koerner 1997). This picture is complicated, however, by results of recent surveys: most T Tauri stars are in binary or multiple systems (Ghez et al. 1993; Leinert et al. 1993). On average, millimeter-wave flux densities are reduced for T Tauri binaries with separations between 1 and 100 AU as compared to T Tauri stars in single or wide binary systems (Jensen et al. 1994; 1996; Osterloh & Beckwith 1995). This range of separations largely encompasses the distribution of radii observed for dust disks around young, low-mass stars and emphasizes the likelihood of a direct impact of companions on circumstellar disks. By determining the spatial distribution of dust in binary systems with separations of several tens to 100 AU, the nature of disk/companion interactions can be investigated empirically.

T Tauri was identified initially as a prototype of a class of pre-main-sequence stars (cf. Bertout 1989 and references therein) and discovered to be a binary in the infrared (Dyck et al. 1982). The optically-obscured companion, T Tau S, is located $0''.7$ south of the visible star T Tau N, corresponding to a projected separation of 100 AU at the 140 pc distance of the Taurus-Auriga dark cloud (Wichmann et al. 1997). Both sources are detected at 2 and 6 cm accompanied by a bridge of connecting emission (Schwartz et al. 1986). Together with proper motion studies (Ghez et al. 1995), the morphology of this emission strongly suggests that the system is physically bound. T Tau is also associated with a substantial mass of dust, as evidenced by polarized nebulosity at infrared wavelengths (Weintraub et al. 1992) and by one of the highest $\lambda = 1$ mm luminosities among young stars (Adams et al. 1990; Beckwith et al. 1990).

Although T Tau N is at least 7 magnitudes brighter than T Tau S at optical wavelengths (Stapelfeldt et al. 1998), the infrared luminosity of the system is dominated by emission from T Tau S (Ghez et al. 1991). Similar instances of differential extinction are found in a handful of other “Infrared Companion” (IRC) systems and have led to speculation about the precise nature of their origin. Competing IRC models invoke different roles for the interaction between the companions and the distribution of surrounding dust and gas. Observations of the thermal dust emission at millimeter wavelengths can be used to determine the mass distribution. Nearly all such observations carried out thus far, however, do not have the spatial resolution needed to discriminate between a circumbinary disk or envelope and circumstellar disks around either component. Both components of T Tau are

thought to have circumstellar disks based on their infrared excesses, but these observations are sensitive primarily to temperature and do not provide a good measure of the dust *mass* distribution. The highest resolution mm-wave image available to date was obtained recently by Hogerheidje et al. (1997) and suggests that the 1 mm continuum emission is dominated by radiation from T Tau N, although the synthesized beam in their map (FWHM $0''.8$) is slightly larger than the binary separation.

To ascertain the respective masses of any circumstellar disks around the components of T Tau, long-wavelength measurements of optically thin dust emission must be carried out at a spatial resolution that unambiguously separates the respective contributions of the binary components. Observations at $\lambda = 3$ mm probe the mass of the densest material and are ideal for distinguishing compact circumstellar dust from that of a surrounding envelope. They are also important in distinguishing between free-free and thermal dust emission. Accordingly, we have used the new long baseline capability of the BIMA mm-array⁴ to make high resolution 3 mm continuum observations of T Tau.

2. Observations and Results

Observations of T Tau at $\lambda = 2.8$ mm were carried out from 1996 December to 1997 March with the 9-element BIMA array. Continuum emission was measured in an 800 MHz bandwidth centered at 108 GHz. Data were taken with the array in the A, B, and C configurations, providing baseline coverage from 2.1 k λ to 420 k λ with sensitivity to emission on size scales up to $\sim 60''$. Interleaved observations of a nearby quasar, 0431+206, were included as a check on the phase de-correlation on long baselines. The phase calibrator was 0530+135, with an assumed flux of 3.1 Jy during A array. Data were calibrated and mapped using the Miriad package. A map of 0431+206 yielded an image of a point source, indicating little atmospheric degradation of the resolution in the observations of T Tau.

An aperture synthesis image of T Tau was constructed with data from the A array alone (the longest baselines) and is displayed in Figure 1. The beam size is $0''.59 \times 0''.39$ at a position angle of 48° . It is clearly evident that the compact 3 mm emission arises from circumstellar material surrounding T Tau N only. Peak emission of 32 mJy beam⁻¹ is centered at RA(J2000) 04:21:59.424 and Dec(J2000) 19:32:06.41 with an absolute positional uncertainty of $\sigma = \pm 0''.07$ as determined from observations of 0431+206. The peak position is within 1.6σ of the Hipparcos coordinates for T Tau N, but 7.8σ distant from the position

⁴The BIMA array is operated by the Berkeley Illinois Maryland Association with funding from the National Science Foundation.

of T Tau S. The emission is resolved with an approximate deconvolved source size of $0''.45 \times 0''.32$ (FWHM) (63×45 AU) at PA 19° , assuming an elliptical Gaussian shape. The integrated flux density, 50 ± 6 mJy (where the uncertainty is dominated by the flux calibration error), is consistent with the 100 GHz value measured at lower resolution by Momose et al. (1996), 48 ± 7 mJy.

No emission is detected at the position of T Tau S above the 3σ upper limit of 9 mJy beam^{-1} , and no circumbinary emission is apparent. The integrated flux density detected in the compact C array is no greater than that for A array. Since the C array observations are most sensitive to emission on larger spatial scales, up to $60''$, the absence of detectable excess emission implies that the majority of continuum emission detected in a $1'$ aperture at $\lambda = 3$ mm originates from a circumstellar region around T Tau N. The 3σ upper limit on circumbinary emission, accounting for thermal noise and flux calibration errors, is 17 mJy.

Our measurement of the 108 GHz flux density from T Tau N is plotted in Figure 2 together with high-resolution measurements at 43 GHz ($\lambda = 7$ mm) (Koerner et al. 1998), 267 GHz ($\lambda = 1$ mm) and 357 GHz ($\lambda = 0.8$ mm) (Hogerheidje et al. 1997). All four points can be fitted by a single power-law curve with $\chi^2 = 1.8$ and goodness of fit 0.4. The best-fit spectral index $\alpha = d(\log(F_\nu))/d(\log(\nu))$ is 2.30 ± 0.1 . This value is in good agreement with those from disks around single T Tauri stars and consistent with thermal emission from large circumstellar dust grains (Beckwith & Sargent 1991; Mannings & Emerson 1994; Koerner et al. 1995), suggesting that the continuum emission from T Tau N has a single origin in thermal dust emission along the entire wavelength range from $\lambda = 1$ to 7 mm.

We argue that the 3mm emission arises from a circumstellar disk around T Tau N. The spectral slope is consistent with radiation from dust grains (see Koerner et al. 1998 for a more stringent limit on the possible contribution of free-free or gyrosynchrotron emission). The star is detected optically, even though the lower limit to the dust mass is high; if the dust were distributed in a uniform density sphere with a size given by the A array fit, the extinction to the star would be $A_V \sim 1000$.

3. Circumstellar disk models for T Tau N

3.1. Model description

To refine estimates of the parameters of dust around T Tau N, we fit the visibility amplitudes directly with a model of a circumstellar disk. While computationally intensive, fitting in the visibility plane rather than the image plane avoids the non-linear process of deconvolution and allows the instrumental errors to be included in a consistent manner.

Our disk model is thin and circularly symmetric with a flux from an annular region at radius r given by

$$dS_\nu(r) = \frac{2\pi \cos \theta}{D^2} B_\nu(1 - e^{-\tau}) r dr, \quad (1)$$

where B_ν is the Planck function, D is the distance, and θ the inclination angle. Flared disks have been invoked to explain the flat infrared spectral indices of some T Tauri stars (Kenyon & Hartmann 1987); however, the effects due to flaring are not important at these long wavelengths (Chiang & Goldreich 1997). The visibility amplitude V at uv -distance η is calculated with a Hankel transform,

$$V(\eta) = 2\pi \int S_\nu(r) J_0(2\pi\eta r/D) r dr, \quad (2)$$

where J_0 is the Bessel function. The inner radius is set by the dust destruction temperature (2000 K); the exact value has little effect on the millimeter flux density. The temperature, surface density and dust opacity are described by power-law relations: $T(r) = T_{10 \text{ AU}}(r/10 \text{ AU})^{-q}$, $\Sigma(r) = \Sigma_{10 \text{ AU}}(r/10 \text{ AU})^{-p}$, and $\kappa_\nu = \kappa_o(\nu/\nu_o)^\beta$. Due to its dependence on the product of surface density and dust opacity, the optical depth scales with the corresponding power-law exponents in radius and frequency,

$$\tau(r, \nu) = \frac{\Sigma \kappa_\nu}{\cos \theta} \equiv \tau_{10 \text{ AU}} \left(\frac{r}{10 \text{ AU}} \right)^{-p} \left(\frac{\nu}{\nu_o} \right)^\beta. \quad (3)$$

The reference value for κ_o is $0.1 \text{ g}^{-1} \text{ cm}^2$ at $\nu_o = 1200 \text{ GHz}$ ($\lambda = 250 \text{ }\mu\text{m}$; Hildebrand 1983).

Eight parameters were varied in the model-data comparison: $T_{10 \text{ AU}}$, q , $\tau_{10 \text{ AU}}$, p , β , r_{out} , θ , and α , the position angle of the disk on the sky. In addition to the 3 mm visibilities, those measured at 1 mm by Hogerheidje et al. (1997) were used together with the 7 mm flux density (Koerner et al. 1998). The IRAS 100 μm flux of 120 Jy (Ström et al. 1989) was included as an upper limit. For each value of θ and α , the u and v coordinates for each visibility were de-projected to those of a face-on disk, then binned in annuli of de-projected uv -distance for comparison to model values calculated by Eqn. 2. Over 5 million models were compared to the data within an 8-dimensional grid in parameter space. Logarithmic grid spacings were used for the temperature, optical depth and outer radius.

To quantitatively assess the reliability of estimates of properties of a disk around T Tau N, we calculate the probability distribution for each parameter over the entire range of models. A detailed description of this Bayesian approach is given in Lay et al. (1997). Given the data, the probability of a model with a particular set of parameter values is proportional to $e^{-\chi^2}$ where χ^2 is the standard squared difference between data and model, weighted by the uncertainty in the data. A systematic error in overall flux calibration was accounted for by normal weighting of a range of model flux scalings with 1σ corresponding

to a 10% difference in flux. The final probability for a given model was taken as the sum of probabilities over all flux scalings and multiplied by a factor of $\sin \theta$ to account for the fact that edge-on disks are more likely than face-on in a randomly oriented sample. Finally, the relative likelihood of each parameter value was calculated by adding the probabilities of all models with that parameter value.

3.2. Parameter results

The resulting probability distributions for the disk parameters are given below. The ranges considered for $T_{10 \text{ AU}}$, $\tau_{10 \text{ AU}}$, and r_{out} were sufficiently wide to bracket all values with significant probability. Parameters values quoted are at the median of the probability distribution with an error range encompassing 68% of the total probability. However, it is important to keep in mind that the distribution is not Gaussian.

The disk outer radius is $r_{out} = 41_{-14}^{+26}$ AU (Figure 3). The probability that it exceeds the projected binary separation (100 AU) is only 3%. Models with large outer radii generally have higher values of p and lower values of $\tau_{10 \text{ AU}}$. The value for the dust mass opacity index, $\beta = 0.53_{-0.17}^{+0.27}$ (Figure 3), is consistent with values measured for circumstellar disks around T Tauri stars (Beckwith & Sargent 1991; Koerner et al. 1995). There is an 85% probability that $\beta \geq 0.30$, the value calculated by assuming optically thin emission ($S_\nu \propto \nu^{2+\beta}$) and fitting a straight line to the 7, 3, and 1 mm fluxes. As discussed below, this implies that at least some of the emission is optically thick. There is some correlation between models with high values of β and those with high τ and low T . The temperature, $T_{10 \text{ AU}} = 26_{-13}^{+34}$ K, and $\lambda = 3$ mm optical depth, $\tau_{10 \text{ AU}} = 0.50_{-0.36}^{+0.83}$, are not as tightly constrained as r_{out} . Although many models have $\tau > 1$ at 10 AU, most (89%) radiate more than half their total emission in an optically thin regime. Note that for an optically thin disk in the Rayleigh-Jeans regime, Eqn. 1 becomes degenerate in T and τ . Consequently, temperature and optical depth are anti-correlated for $\tau < 0.5$ at 10 AU. The data do not narrowly constrain values for q , p , θ or α . The ranges used for p and q were $p=0.5\text{--}2.0$ and $q=0.4\text{--}0.75$. Steeper density profiles are slightly favored over shallow ones; the probability that p is ≥ 1.5 is 65%. The lack of preferred values for p and q is largely due to the degeneracy of p and q for optically thin emission.

It may be possible to constrain the disk parameters further by including data from additional wavelengths. Mid-infrared flux densities are often used to determine q and T_o , for example. We chose not to include these data, however, because the mid-infrared flux traces material within a few AU of the star, while the millimeter data is sensitive mainly to material tens of AU away. The simple power-law relations assumed in the model may not

be valid over such a large range of disk radii and physical conditions.

The disk model masses, weighted by the model probabilities, were binned to derive a median value $\log(M_D/M_\odot) = -2.4_{-0.6}^{+0.7}$ (Figure 3). The wide range in mass is due largely to the range of τ values that fit the data. For a given 3 mm flux, disks with higher mass correspond to those with higher τ and β . The median value for the disk mass, $M_D = 4 \times 10^{-3} M_\odot$, is toward the low end of disk masses typically derived for classical T Tauri stars (e.g. Beckwith et al. 1990). We note, however, a large dependence of mass estimates on values assumed for the other parameters. Beckwith et al. assumed $\beta = 1$ and an outer radius of 100 AU. If we consider only models with $\beta \geq 0.75$ and an outer radius > 50 AU, the median mass increases to $10^{-2} M_\odot$, similar to the minimum mass solar nebula.

4. Discussion

It has been conjectured that the formation of planetary systems arises from the collapse of protostellar clouds which rotate more slowly than clouds from which binaries form (Safronov & Ruzmaikina 1985). This, in turn, raises the possibility that planetary systems may fail to form in the binary environment. In contrast, our observations and modeling demonstrate that a substantial mass of material, with size like that of the solar system, can exist around a star in a binary system with separation not less than 100 AU. This material constitutes a large reservoir available to planet-forming processes; the low value of the mass opacity index, $\beta = 0.53$, further suggests that the formation of larger grains may already be underway as a first step toward planetesimal formation (Beckwith & Sargent 1991; Mannings & Emerson 1994; Koerner et al. 1995).

Our observations rule out a greater circumstellar mass of dust around T Tau S—whether in an edge-on circumstellar disk or compact spherical envelope—as a simple explanation for the origin of increased extinction along the line of sight to T Tau’s infrared companion. Due largely to the low optical depth of dust continuum emission at $\lambda = 3$ mm, however, the true source of extra extinction is not identified unambiguously. Our estimate of the outer radius is smaller than the projected separation between T Tau N and S and suggests that a disk around T Tau N does not obscure T Tau S. However, we did not consider models with an exponential density profile at the outer edge like that of Hogerheidje et al. (1997). We note that since $\kappa(500 \text{ nm})/\kappa(3 \text{ mm}) \sim 10^3\text{--}10^4$ (e.g., Pollack et al. 1994), the material that provides the extinction toward T Tau S could easily be undetectable at 3 mm. Thus, our data are consistent either with obscuration of T Tau S by tenuous outer regions of the T Tau N disk or with truncation of the T Tau N disk by T Tau S as discussed below.

If the binary components are in a bound orbit, as suggested by their common proper motion, the distribution of circumstellar material at the outer edge of the disk will be affected by the gravitational influence of the companion. In models of disk/companion interactions, the size of the circumstellar disk depends on the mass ratio of the stars and their separation (Papaloizou & Pringle 1977, Artymowicz & Lubow 1994). The radius of the circumprimary disk typically ranges from 0.3 to 0.4 times the separation for mass ratios of 1 to 0.3 and circular orbits. If the orbital plane of the system is viewed nearly face-on and the binary separation is 100–110 AU, the tidal disk radius would be 30–40 AU. The disk size estimated from modeling our observations, $27 < R < 67$ AU, is consistent with the range of values predicted for tidal truncation. If tidal truncation has occurred and we are seeing the true size of the disk in our maps, then the disk around T Tau N is not obscuring T Tau S. However, high-resolution observations at sub-millimeter wavelengths or in molecular transitions that better trace low-column-density material are needed to adequately solve this problem.

Finally, we point out that the disk around T Tau N is similar to those observed around some single low-mass stars, regardless of the reliability of model assumptions that lead to an estimate of the absolute value of its mass and size, since the millimeter-wave flux from T Tauri is among the brightest measured from a large sample of young low-mass stars (cf. Beckwith et al. 1990, Osterloh & Beckwith 1995), and the nominal FWHM size of the emission is similar to that of single-star disks for which sufficiently high-resolution observations have been carried out (e.g. Lay et al. 1994; Mundy et al. 1996). If the largest disks around T Tauri stars typically yield planetary systems like our own, it is plausible that the disk around T Tau N will too, in spite of the presence of a companion at a distance of 100 AU or greater. Since the majority of pre-main-sequence stars are in multiple systems, the possibility of planetary formation in binaries like T Tauri invites consideration of the likelihood that a non-negligible fraction of binary stars contribute substantially to the estimated fraction of stars that possess planetary systems.

We are grateful to M. Hogerheidje for allowing us to use the 1 mm data. We thank L. Looney and L. Mundy for help with observing and O. Lay for helpful discussions. RLA acknowledges support from the Miller Institute for Basic Research in Science. ELNJ and DWK gratefully acknowledge support from the National Science Foundation’s Life in Extreme Environments Program through grant AST-9714246.

REFERENCES

- Adams, F.C., Emerson, J.P., and Fuller, G.A., 1990, *ApJ*, 357, 606
- Artymowicz, P. and Lubow, S.H., 1994, *ApJ*, 421, 651
- Beckwith, S.V.W., Sargent, A.I., Chini, R.S., and Güsten, R., 1990, *AJ*, 99, 924
- Beckwith, S.V.W. and Sargent, A.I., 1991, *ApJ*, 381, 250
- Beckwith, S.V.W. and Sargent, A.I., 1996, *Nature*, 383, 189
- Bertout, C., 1989, *ARA&A*, 27, 351
- Chiang, E.I., and Goldreich, P., 1997, *ApJ*, 490, 368
- Dyck, H.M., Simon, T. and Zuckerman, B., 1982, *ApJ*, 255, 103
- Ghez, A.M., Neugebauer, G., Gorham, P.W., Haniff, C.A., Kulkarni, S.R., Matthews, K., Koresko, C., and Beckwith, S., 1991, *AJ*, 102, 2066
- Ghez, A.M., Neugebauer, G., and Matthews, K., 1993, *AJ*, 106, 2005
- Ghez, A.M., Weinberger, A.J., Neugebauer, G., Matthews, K. and McCarthy, D.W., 1995, *AJ*, 110, 753
- Hildebrand, R.H., 1983, *QJRAS*, 24, 267
- Hogerheidje, M.R., van Langevelde, H.J., Mundy, L.G., Blake, G.A., and van Dishoeck, E.F., 1997, *ApJ*, 490, L99
- Jensen, E.L.N., Mathieu, R.D., and Fuller, G.A., 1994, *ApJ*, 429, L29
- Jensen, E.L.N., Mathieu, R.D., and Fuller, G.A., 1996, *ApJ*, 458, 312
- Kenyon, S.J., and Hartmann, L., 1987, *ApJ*, 323, 714
- Koerner, D.W., 1997, *OLEB*, 27, 157
- Koerner, D.W., Chandler, C.J., and Sargent, A.I., 1995, *ApJ*, 452, L69
- Koerner, D.W., Jensen, E.L.N., Ghez, A.M., and Mathieu, R.D., 1998, *ApJ*, submitted
- Lay, O.P., Carlstrom, J.E., Hills, R.E., and Phillips, T.G., 1994, *ApJ*, 434, 75
- Lay, O.P., Carlstrom, J.E., and Hills, R.E., 1997, *ApJ*, 1997, 489, 917
- Leinert, Ch., Weitzel, N., Zinnecker, H., Christou, J., Ridgway, S. T., et al., 1993, *A&A*, 278, 129
- Mannings, V., and Emerson, J.P., 1994, *MNRAS*, 267, 361
- Momose, M., Ohashi, N., Kawabe, R., Hayashi, M., and Nakano, T., 1996, *ApJ*, 470, 1001

- Mundy, L.G., Looney, L.W., Erickson, W., Grossman, A., Welch, W.J., Forster, J.R., Wright, M.C.H., Plambeck, R.L., Lugten, J., and Thorton, D.D., 1996, *ApJ*, 464, 169
- Osterloh, M. and Beckwith, S.V.W., 1995, *ApJ*, 439, 288
- Papaloizou, J.C.B., and Pringle, J.E., 1977, *MNRAS*, 181, 441
- Pollack, J.B., Hollenbach, D., Beckwith, S., Simonelli, D.P., Roush, T., and Fong, W. 1994, *ApJ*, 421, 615
- Safronov, V.S., and Ruzmaikina, T.V., 1985, in *Protostars and Planets II*, (ed. D.C. Black and M.S. Matthews), Tucson: University of Arizona Press, p. 959
- Schwartz, P.R., Simon, T. and Campbell, R., 1986, *ApJ*, 303, 233
- Shu, F.H., Najita, J., Galli, D., Ostriker, E., and Lizano, S., 1993, in *Protostars and Planets III*, (ed. E.H. Levy and J.I. Lunine), Tucson: University of Arizona Press, p. 3
- Skinner, S.L. and Brown A., 1994, *AJ*, 107, 1461
- Strom, K.M., Strom, S.E., Edwards, S., Cabrit, S., and Skrutskie, M.F., 1989, *AJ*, 97, 1451
- Weintraub, D.A., Kastner, J.H., Zuckerman, B. and Gatley, I., 1992, *ApJ*, 391, 784
- Wichmann, R., Bastian, U., Krautter, J., Jankovics, I. and Ruciński, S., 1997, *MNRAS*, in press

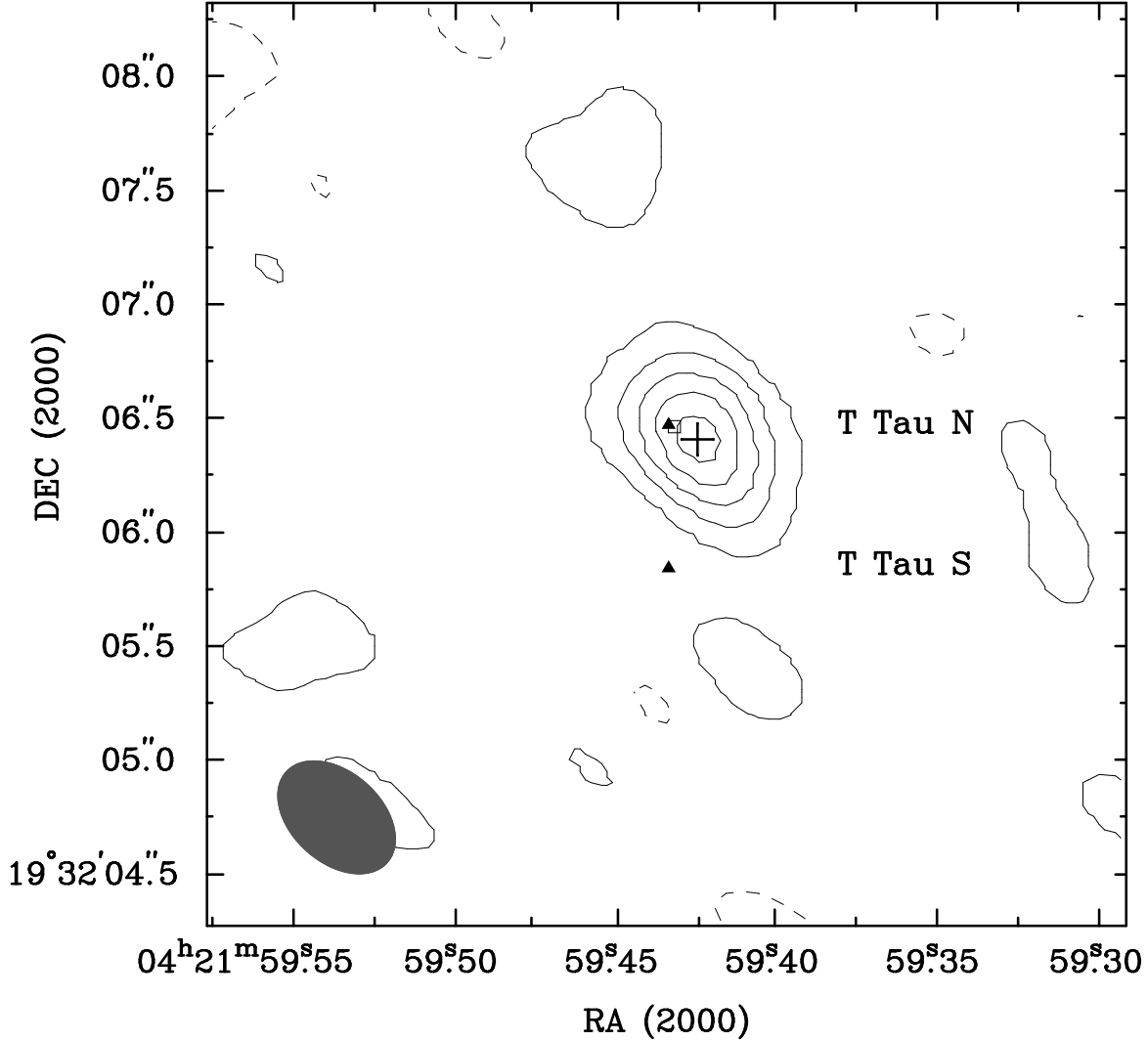


Fig. 1.— The 108 GHz continuum emission using only the longest spacing array. The beam size is $0''.59 \times 0''.39$ at a position angle of 48° . The peak flux is 32 mJy/beam and the RMS is 3.1 mJy/beam. The contour levels plotted are 2σ . The size of the error bars on the millimeter emission center position (cross) represents the absolute positional uncertainty for the millimeter image of $0''.07$. The filled triangles mark the radio positions of T Tau N and S from Skinner & Brown (1994), where the error bars (which do not include any possible systematic errors) are within the symbol. The open square marks the optical position of T Tau N from Hipparcos. All positions were adjusted to epoch 1997.0 using a proper motion of $\mu_{\alpha\cos\delta} = 0''.015 \text{ yr}^{-1}$ and $\mu_\delta = -0''.012 \text{ yr}^{-1}$ (Hipparcos).

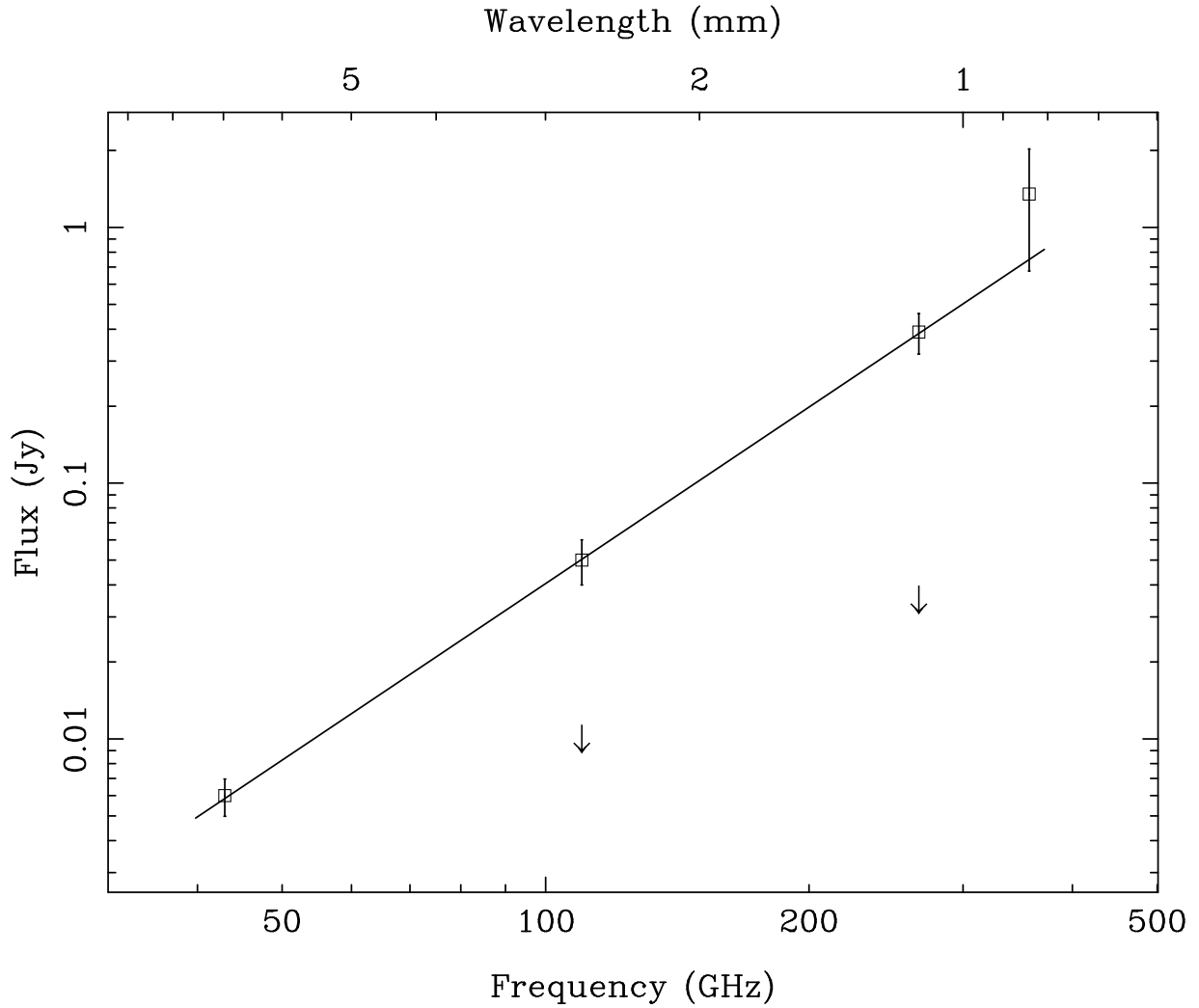


Fig. 2.— Millimeter and sub-millimeter fluxes for T Tau N (squares) and 3σ upper limits (arrows) for T Tau S. The 267 GHz ($\lambda=1$ mm) and 357 GHz ($\lambda=0.8$ mm) fluxes are from Hogerheidje et al. (1997). The 43 GHz ($\lambda=7$ mm) flux is from Koerner et al. (1998). The solid line fit is plotted with $\alpha=d(\log(F_\nu))/d(\log(\nu))$ of 2.3.

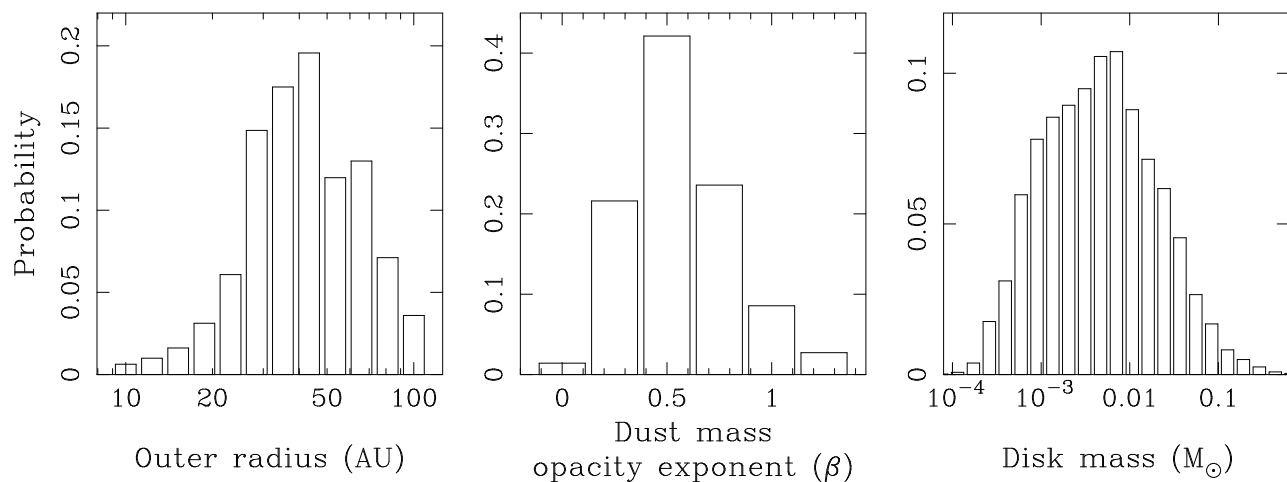


Fig. 3.— The probability distributions for the disk outer radius, dust mass opacity exponent and derived disk mass. The likelihood of each parameter value was calculated by summing the probabilities for models with all possible values of the remaining parameters. The relative value of the probability is more important than the absolute value, which depends on the number of parameter values used in the calculations.